INFECTION AND IMMUNITY, June 2009, p. 2530–2543 Vol. 77, No. 6
0019-9567/09/$08.00+0 doi:10.1128/IAI.00905-08

Bacillus anthracis Edema Toxin Suppresses Human Macrophage Phagocytosis and Cytoskeletal Remodeling via the Protein Kinase A and Exchange Protein Activated by Cyclic AMP Pathways▽

Linsey A. Yeager,[1]* Ashok K. Chopra,[1,2] and Johnny W. Peterson[1,2]

Department of Microbiology and Immunology[1] and Center for Biodefense and Emerging Infectious Diseases and Sealy Center for Vaccine Development,[2] University of Texas Medical Branch, Galveston, Texas 77555

Received 22 July 2008/Returned for modification 8 September 2008/Accepted 14 March 2009

***Bacillus anthracis*, the etiological agent of anthrax, is a gram-positive spore-forming bacterium. It produces edema toxin (EdTx), a powerful adenylate cyclase that increases cyclic AMP (cAMP) levels in host cells. Because other cAMP-increasing agents inhibit key macrophage (MΦ) functions, such as phagocytosis, it was hypothesized that EdTx would exhibit similar suppressive activities. Our previous GeneChip data showed that EdTx downregulated MΦ genes involved in actin cytoskeleton remodeling, including protein kinase A (PKA). To further examine the role of EdTx during anthrax pathogenesis, we explored the hypothesis that EdTx treatment leads to deregulation of the cAMP-dependent PKA system, resulting in impaired cytoskeletal functions essential for MΦ activity. Our data revealed that EdTx significantly suppressed human MΦ phagocytosis of Ames spores. Cytoskeletal changes, such as decreased cell spreading and lowered F-actin content, were also observed for toxin-treated MΦs. Further, EdTx altered the protein levels and activity of PKA and exchange protein activated by cAMP (Epac), a recently identified cAMP-binding molecule. By using PKA- and Epac-selective cAMP analogs, we confirmed the involvement of both pathways in the inhibition of MΦ functions elicited by EdTx-generated cAMP. These results suggested that EdTx weakened the host immune response by increasing cAMP levels, which then signaled via PKA and Epac to cripple MΦ phagocytosis and interfered with cytoskeletal remodeling.**

Bacillus anthracis, the etiological agent of anthrax, is a category A select agent that has received renewed public and scientific interest following its reemergence as a biological threat in 2001. The organism is a gram-positive spore-forming bacterium that can enter the host via inhalation or ingestion or through abrasions in the skin barrier. The inhalational form of anthrax is the deadliest, and without treatment, it often quickly advances to fatal systemic infection (21, 25).

The virulence of *B. anthracis* is partly determined by its two plasmids, pX01 and pX02. Plasmid pX02 carries genes for the biosynthesis and degradation of the poly-D-glutamic acid capsule. Strains of *B. anthracis* lacking the capsule have noticeably reduced virulence in animal models (54). Plasmid pX01 harbors a pathogenicity island that codes for the three components of the anthrax toxins: lethal factor (LF), edema factor (EF), and protective antigen (PA). PA binds the cell surface receptors ANTXR1 (TEM8) and ANTXR2 (CMG2) (10, 57) and forms pores in the lipid bilayers of target cells (1). After PA heptamerizes on the cell surface, LF and EF enzyme moieties are delivered to the mammalian cytosol, where they exert their toxic activities. The majority of information regarding *B. anthracis* lethality has been gained from studies with lethal toxin (LeTx), which is comprised of LF and PA. LF is a zinc-dependent protease whose major function is proteolytic cleavage of mitogen-activated protein kinase kinase family members. This results in attenuation of the host immune response and apoptosis of murine and human macrophages (MΦs) and endothelial cells (36, 39, 53).

Edema toxin (EdTx) is formed by a combination of EF and PA. EF is a calcium- and calmodulin-dependent adenylate cyclase that causes a prolonged increase in intracellular cyclic AMP (cAMP) within numerous types of target cells (43). EF is at least 1,000-fold more active in cAMP production than are host adenylyl cyclases (22, 44, 60). Interestingly, mice died more rapidly after receiving lower doses of EdTx than of LeTx (23). Extensive animal tissue lesions were observed, and death was likely due to multiorgan failure. Microarray data published previously by our group revealed changes in murine MΦ genes involved in inflammatory responses, regulation of apoptosis, immune cell activation, and transcription regulation as early as 3 h post-toxin treatment, emphasizing the powerful activity of the toxin (17). However, the downstream effects of EdTx activity have not been studied extensively, and it is still unclear how EdTx sabotages host defenses.

Other agents that elevate cAMP concentrations within MΦs result in inhibition of an array of MΦ functions, such as phagocytosis, migration, spreading, adhesion, superoxide production, and bacterial killing (12, 55, 59). Indeed, studies examining the effect of EdTx on human neutrophils showed that the phagocytic capacity and oxidative burst of these cells were reduced (50, 63). Additionally, EdTx treatment impaired human MΦ migration. Rossi et al. (56) attributed this phenomenon to a reduction in chemokine receptor signaling following toxin treatment. However, we hypothesized that a second mechanism potentially responsible for reduced motility was impairment of the MΦ cytoskeleton by EdTx.

EdTx treatment of the murine MΦ cell line RAW 264.7

* Corresponding author. Mailing address: 301 University Blvd., Galveston, TX 77555-0610. Phone: (409) 266-6824. Fax: (409) 747-6869. E-mail: layeager@utmb.edu.

▽ Published ahead of print on 23 March 2009.

elicited significant alterations of multiple genes whose products were vital for proper actin structure and rearrangement, including an important signaling molecule that bound cAMP and modulated the actin cytoskeleton. There was a 2.6-fold upregulation of the regulatory subunit of protein kinase A (PKA) (17) in toxin-treated MΦs. The cAMP-dependent PKA is involved in nearly every family of the cytoskeletal network, including microtubules, intermediate filaments, and actin microfilaments. PKA plays a dichotomous role, as some hallmarks of cell migration and cytoskeletal assembly require PKA activity (activation of Rac, Cdc42, and microfilament assembly), while others are inhibited by it (activation of Rho and p21-activated kinase, VASP interaction, and actin polymerization) (reviewed in reference 30).

Although the effects of cAMP were once thought to be solely transduced by PKA, exchange protein activated by cAMP (Epac) has recently been implicated as a member of the cAMP signaling cascade that acts independently of PKA (20, 38). Epac belongs to a family of guanine exchange factors that directly activate the small GTPase Rap1 and participates in versatile pathways, among which are modulation of integrins associated with the actin cytoskeleton and regulation of actin dynamics. Previous microarray analysis identified an 8.2-fold downregulation of the Epac-related activator of Rap1, Rap guanine nucleotide exchange factor 5 (RapGEF5), following a 6-h EdTx treatment in murine MΦs (17). Furthermore, it was recently shown that human endothelial cells treated with EdTx underwent cytoskeletal changes and exhibited impaired chemotaxis due to activation of the Epac pathway (28).

Thus, in order to further examine the role of EdTx during anthrax pathogenesis in the human host, we explored the hypothesis that EdTx treatment leads to alteration of the cAMP-dependent PKA and/or Epac system, resulting in impaired cytoskeletal functions of host MΦs that are essential for their migration and phagocytosis. Indeed, EdTx treatment elicited cytoskeletal changes in human MΦs, as well as suppressed their phagocytic activity. The use of chemical cAMP analogs with specificity for PKA or Epac showed that both pathways were targeted in MΦs by EdTx-generated cAMP. These results identified a new role for EdTx and provided further evidence that EdTx weakened the host immune response by impairing one of the major players during anthrax pathogenesis, the MΦ.

MATERIALS AND METHODS

Cell line and reagents. Human HL-60 cells (ATCC, Manassas, VA) were maintained in Iscove's Modified Dulbecco's medium with 20% fetal bovine serum and penicillin/streptomycin. To differentiate these cells into MΦs, 200 nM phorbol 12-myristate 13-acetate (PMA) (Sigma, St. Louis, MO) was added where indicated for 24 h. Differentiation was confirmed by adherence, morphological changes, increased expression of CD11b, and phagocytosis of *Escherichia coli*-conjugated particles (data not shown). Upon treatment with PMA, these cells became terminally differentiated and no longer continued to divide.

Before each experiment, the PMA-containing medium was removed and the cells were washed with phosphate-buffered saline (PBS). Purified *B. anthracis* EF and PA were provided by the Biodefense and Emerging Infections Research Resources Repository (Manassas, VA) and reconstituted with molecular-grade water. Aliquots of the toxins were stored at −80°C, and the concentrations used were 1.25 μg/ml EF and 5 μg/ml PA in all cases, unless otherwise indicated. DHR 123 and Alexa Fluor 594 phalloidin were purchased from Molecular Probes (Eugene, OR). PMA, lipopolysaccharide (LPS), cytochalasin B, phosphatase inhibitor cocktail 1, and protease inhibitor cocktail were purchased from Sigma. Horseradish peroxidase (HRP)-conjugated GAPDH (glyceraldehyde-3-phosphate dehydrogenase) antibody and rabbit anti-Epac were purchased from Santa Cruz (Santa Cruz, CA). Mouse anti-PKA RIIα was from BD Biosciences (San Jose, CA). 8-(4-Chlorophenylthio)-2′-*O*-methyladenosine-3′,5′-cAMP (8-CPT-2Me), N_6-benzoyladenosine-3′,5′-cAMP (6-Bnz-cAMP), and myristoylated PKI (mPKI), each purchased from Biolog Life Sciences Institute (Bremen, Germany), were reconstituted with molecular-grade water, and aliquots were stored at −20°C (215 mM, 200 mM, and 1 mg/ml, respectively).

Isolation and culture of primary human MΦs. First, monocytes were purified from buffy coats as described previously (9). Briefly, human peripheral blood monocytic cells were collected following Ficoll-Paque Plus (GE Healthcare, Piscataway, NJ) density centrifugation. The monocytes were isolated by negative selection using a magnetic-column separation system (StemCell Technologies, Vancouver, Canada). The monocytes were then differentiated into alveolar-like MΦs as previously described (5, 40). The monocytes were resuspended in RPMI 1640 at a concentration of 2.5×10^5 per ml in six-well tissue culture plates and cultured with granulocyte-MΦ colony-stimulating factor (GM-CSF) (500 units/ml; PeproTech, Rocky Hill, NJ) and 10% heat-inactivated fetal bovine serum for 7 days at 37°C in a CO_2 incubator.

Spore preparation. Spores were prepared as previously described (52). Briefly, *B. anthracis* strain Ames was inoculated in Schaeffer's sporulation medium (pH 7.0), consisting of 16 g Difco Nutrient Broth, 0.5 g $MgSO_4 \cdot 7H_2O$, 2.0 g KCl, and 16.7 g MOPS (morpholinepropanesulfonic acid) per liter. Before inoculation, the following supplements were added to the medium: 0.1% glucose, 1 mM $Ca(NO_3)_2$, 0.1 mM $MnSO_4$, and 1 μM $FeSO_4$. Cultures were grown at 37°C with gentle shaking (180 rpm) for 48 h, after which sterile distilled water was added to dilute the medium and promote sporulation. After 10 to 11 days of continuous shaking, sporulation was confirmed at >99% via phase-contrast microscopy and a modified Wirtz-Conklin spore stain, and the spores were centrifuged at 630 × *g* at 4°C for 15 min. The spore pellets were then washed four times in Cellgro sterile water (Mediatech, Herndon, VA) and resuspended in sterile water. Subsequently, the spore suspension was layered onto a cushion of 58% Hypaque-76 (GE Healthcare) at a ratio of 1:2.5 by volume. Without being mixed, the tubes were centrifuged at 8,270 × *g* for 45 min at 4°C. The spore pellet was washed twice with sterile water and finally resuspended in PBS. Aliquots of the stock spore suspension were stored at −80°C and freshly diluted in PBS to the desired number of CFU immediately before each experiment. The spore suspensions were homogeneous when examined by phase-contrast microscopy.

cAMP ELISA. MΦs (5×10^5/well) were seeded in triplicate wells per condition and exposed to two concentrations of EdTx, either 0.625 μg/ml EF plus 2.5 μg/ml PA or 1.25 μg/ml EF plus 5 μg/ml PA. Some wells were left untreated, while others received 1 ng/ml LPS, to account for the low levels of LPS in the toxin preparations, or EF or PA alone. A portion of the culture supernatant in each well was saved at time points of 2, 6, and 24 h, followed by lysing of the MΦs in the well with 0.1 M HCl, and a portion of each intracellular lysate was saved. Samples were stored at −80°C until the cAMP enzyme-linked immunosorbent assay (ELISA) kit (Assay Designs, Ann Arbor, MI) was used to measure the cAMP levels of intracellular lysates and extracellular supernatants. The total protein concentration of each well was also measured from these samples in order to express the final data as pmol of cAMP per mg of cellular protein. This experiment was performed independently three times.

Phagocytosis assays. MΦs (5×10^5/well) were seeded in triplicate using 24-well plates and exposed to EdTx for the indicated times. Simultaneously, the cells were infected with Ames spores (multiplicity of infection [MOI] = 5) for 1 h at 37°C with 5% CO_2. The cells were subsequently treated with 100 μg/ml gentamicin for 30 min to kill extracellular bacteria. All wells then underwent multiple washes with PBS to remove extracellular spores. The lysates were serially diluted with PBS, immediately plated on blood agar plates, and incubated at 37°C for 24 to 48 h. Colonies were counted the next day, and phagocytosis was expressed as the number of viable intracellular *B. anthracis* CFU (both dormant and vegetative) recovered per 5×10^5 MΦs.

Additionally, the Vybrant Phagocytosis assay (Molecular Probes) was used and was performed according to the manufacturer's instructions. MΦs (1×10^5/well) were seeded in 96-well plates (quadruplicate wells per condition) and pretreated with EdTx for 3, 6, and 24 h. Controls of untreated cells and LPS (1 to 100 ng/ml)- and cytochalasin B-treated MΦs were also included. Furthermore, some wells received 6-Bnz-cAMP (300 μM), mPKI (25 μM), or 8-CPT-2Me (100 μM) for 1 h. Next, fluorescein isothiocyanate (FITC)-conjugated *E. coli* Bioparticles (Molecular Probes; 100 μl) were added to each well and incubated for 1 h at 37°C. After removal of the Bioparticles, trypan blue was added to quench extracellular fluorescence, and the plate was read with a SpectraMax M5^e plate reader (Molecular Probes) with settings of 480 nm (excitation) and 520 nm (emission).

F-actin content. Similar to the method of Hu et al. (33), 2.5×10^5 MΦs were seeded in quadruplicate wells of 96-well plates and left untreated or treated with EdTx for 2, 6, or 24 h; cytochalasin B (10 μg/ml) for 2 h; or 6-Bnz-cAMP (300

μM), mPKI (25 μM), or 8-CPT-2Me (100 μM) for 1 h. Some wells received a combination of EdTx and mPKI simultaneously for 6 h. FITC-labeled *E. coli*-conjugated particles were then added to each well for 1 h to elicit cellular motility and phagocytosis. Host cells were subsequently washed, fixed with 3.7% paraformaldehyde, and permeabilized with 0.1% Triton X-100. After the cells were washed again, Alexa Fluor 594-phalloidin was added to the cells for 30 min before several final washes. A small volume of PBS was left in each well, and the plate was read on a plate reader with settings of 590 nm (excitation) and 617 nm (emission). This experiment was repeated three times for each MΦ type, and one representative experiment was graphed.

Immunofluorescence and cell spreading. The immunofluorescence and cell-spreading experiment followed the protocol of Lasunskaia et al. (42). HL-60 MΦs were seeded on glass coverslips and pretreated with EdTx (2, 6, 12, and 24 h), cytochalasin B (1 h), or EF or PA alone (24 h). Next, FITC-conjugated *E. coli* particles were added as a phagocytic stimulus for an additional hour. Coverslips were washed in PBS and then permeabilized with 0.1% Triton X-100 for 5 min. Following another PBS wash, host cells were fixed with 3.7% paraformaldehyde for 30 min at room temperature. Finally, MΦs were washed and labeled with Alexa Fluor 594-conjugated phalloidin for 30 min before being mounted with SlowFade Gold with DAPI (4′,6′-diamidino-2-phenylindole) mounting solution (Molecular Probes). The coverslips were viewed with an Axioplan II fluorescence microscope, and the images were recorded using an Axiophot 2 dual camera. For quantification of MΦ spreading, ImageJ v1.37 software (NIH, Bethesda, MD) (http://rsb.info.nih.gov/ij/) was employed to measure cellular dimensions. The perimeters of cells in at least five fields of view per slide were manually traced, and the software calculated the area, perimeter, length, and width of each individual cell. The spreading index was expressed as a relation of a mean cell area of EdTx-treated cells compared to control, untreated cells. At least 100 randomly selected cells of each slide were examined by the ImageJ software.

PKA activity assay. For the PKA activity assay, following EdTx or cAMP analog pretreatment, HL-60 cultures grown in 10-cm plates were lysed with the lysis buffer provided with the Omnia PKA Assay (Invitrogen, Carlsbad, CA), along with phosphatase and protease inhibitors. After clarification of the extracts by centrifugation, the lysates were stored at −80°C until analysis. The bicinchoninic acid protein assay (Bio-Rad, Hercules, CA) was performed in order to quantitate the protein levels of each sample, and the PKA assay kit protocol was adhered to for subsequent assessment of kinase activity. Briefly, the reaction was initiated by adding the master mix, i.e., appropriate buffers, ATP, the PKA substrate, and a non-PKA inhibitor cocktail, to 1 μg total protein of the lysates. Fluorescence intensity readings were collected every 2 min for at least 20 min (360 nm [excitation] and 485 nm [emission]). For graphing purposes, the data were expressed as a cell lysate PKA activity curve (relative fluorescence units versus time). These experiments were performed independently three times, and all showed the same trend. Each figure is representative of one particular experiment of the set.

Rap1 pull-down assay and Western blot analysis. To assess Rap1 activation, a pull-down assay followed by Western blot analysis was performed. Heavily seeded HL-60 cultures were grown in 10-cm plates, treated with EdTx or the cAMP analogs for appropriate times, washed once with PBS, and then lysed with small volumes of lysis buffer included in the EZ Detect Rap1 kit (Pierce, Rockford, IL). Following a high-speed spin to pellet cell debris, supernatants were collected and protein quantitation was performed on each sample. Following the manufacturer's instructions, the samples were incubated with glutathione *S*-transferase (GST) fusion protein RNA binding domain (RBD) of RalGDS, a downstream effector of Rap1, immobilized to glutathione beads for 1 h at 4°C with gentle agitation to specifically isolate active (GTP-bound) Rap1. The resin was washed several times with wash buffer before final collection of the sample by centrifugation. Proteins were resolved by sodium dodecyl sulfate-polyacrylamide gel electrophoresis (25 μg protein/lane) and transferred to a nitrocellulose membrane. The latter was probed with a rabbit anti-Rap1 antibody (Pierce; 1:1,000 dilution) overnight at 4°C, followed by the appropriate HRP-conjugated secondary antibody for 1 h at room temperature. Finally, SuperSignal chemiluminescence detection reagent (Pierce) was applied. To ensure that equal amounts of protein were loaded in each lane, cell lysates were also immunoblotted with anti-GAPDH antibodies. In some cases, densitometry (Quantity One; Bio-Rad) was utilized to quantitate each band, and the data were expressed as the change compared to untreated controls. The experiment was performed two times, and the graph shown is an average of the two experiments.

To examine PKA RIIα and Epac levels, Western blot analysis was performed similarly to that described above. However, the treated cells were lysed with RIPA buffer containing phosphatase and protease inhibitors for 1 h on ice. Samples were then subjected to sodium dodecyl sulfate-polyacrylamide gel electrophoresis (20 μg protein/lane) and transferred to nitrocellulose membranes. Next, the membranes were probed with primary antibody for 1 h (1:500 dilution of PKA RIIα or Epac), followed by incubation with the appropriate HRP-conjugated secondary antibodies (Santa Cruz Biotechnology) for 1 h. The membranes were developed as described above, densitometry was performed, and the data were expressed as the change compared to untreated controls. Again, the GAPDH levels of the host cells were examined to ensure equal protein loading. This experiment was performed three times for each antibody, and the average of the three experiments was graphed.

MTT assay. Differentiated HL-60 cells or primary cells were seeded in 96-well plates (2.5×10^5/well) and treated with EdTx (1.25 μg/ml EF plus 5 μg/ml PA) for 2, 6, and 24 h. Controls consisting of untreated cells and those receiving EF or PA alone were included. Next, 10 μl of MTT reagent (3-[4,5-dimethylthiazoyl-2]-2,5-diphenyltetrazolium bromide), included in the MTT Cell Proliferation Assay (ATCC), was added to each well, and the plate was incubated for 2 h at 37°C. Subsequently, 100 μl of the detergent reagent was added per well, and the plate was incubated at room temperature overnight in the dark. Finally, the absorbance was read at 570 nm. Internal controls included wells with no cells (only medium plus MTT reagent and detergent) to detect background absorbance levels. A decrease in absorbance indicated a reduction in cell viability, and the experiment was performed independently three times.

Statistics. As indicated, experiments were performed in either triplicate or quadruplicate and repeated at least three times to ensure reproducibility, or as indicated. Data were expressed as the mean ± standard deviation of the replicates. Differences were considered statistically significant when the P value was <0.05 as determined by one-way analysis of variance (ANOVA), using SigmaPlot software, followed by the Dunnett test, the Student-Newman-Keub test, or Dunn's test where indicated.

RESULTS

EdTx increases cAMP levels in HL-60 MΦs. Experiments in this study were performed with both human primary alveolar-like MΦs and the human promyelocytic cell line HL-60. Human monocytes cultured with GM-CSF differentiated into cells closely resembling alveolar MΦs with respect to morphology (48), expression of cell surface antigens (4, 7), and function (40, 49, 46). Alternatively, HL-60 cells could be differentiated into various cell types depending on the treatment (15). PMA was added for 24 h to differentiate the nonadherent HL-60 cells into adherent MΦ-like cells capable of phagocytosis and bacterial killing (15, 24).

To verify that both MΦ types were susceptible to the activity of EdTx, a cAMP ELISA was performed. HL-60 cells and primary MΦs were exposed to EdTx at two concentrations (either 0.625 μg/ml EF plus 2.5 μg/ml PA or 1.25 μg/ml EF plus 5 μg/ml PA) for 2, 6, and 24 h before extracellular supernatants and intracellular lysates were collected. Both pools were evaluated in order to determine whether the majority of cAMP evoked by EdTx treatment was secreted or contained intracellularly. The phosphodiesterase inhibitor 3-isobutyl-1-methylxanthine (IBMX, 50 μM) was applied during the incubations to prevent intrinsic phosphodiesterase activity from degrading the cAMP. Figure 1 shows that the higher concentration of EdTx significantly increased total cAMP production in both cell types at 6 h, and this effect was further enhanced at 24 h. Therefore, this concentration of EdTx was chosen for all subsequent studies presented here. Controls consisting of EF and PA alone did not evoke significant cAMP production. *E. coli* LPS (1 ng/ml) was also applied to mimic the low levels of LPS contamination found in the toxin; however, it did not elicit cAMP production.

To determine whether EdTx was cytotoxic to the HL-60 and primary MΦs, the MTT assay was used to monitor cell viability following toxin treatment for 2, 6, and 24 h. The results showed

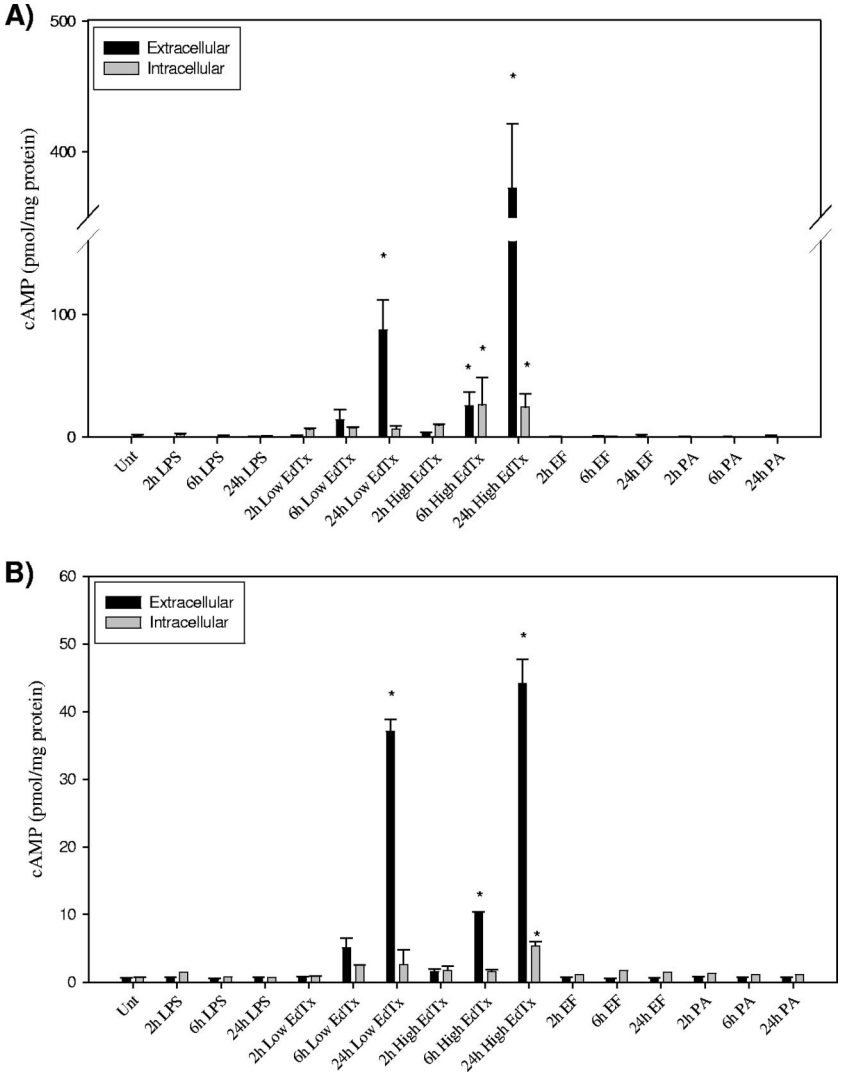

FIG. 1. EdTx increases cAMP levels in human MΦs. HL-60 (A) and primary (B) MΦs in triplicate wells per condition were treated with EdTx at two concentrations (0.625 μg/ml EF plus 2.5 μg/ml PA [Low] and 1.25 μg/ml EF plus 5 μg/ml PA [High]), LPS (1 ng/ml), EF alone (1.25 μg/ml), or PA alone (5 μg/ml) or left untreated. At each time point, extracellular and intracellular samples were collected and analyzed by cAMP ELISA. EF and PA treatments did not result in high levels of cAMP production in either cell type. Each graph shows the averaged results of three independent experiments carried out on triplicate wells ± standard deviations. The asterisks indicate statistical significance ($P < 0.05$) using ANOVA and Dunnett's tests.

that EdTx (1.25 μg/ml EF plus 5 μg/ml PA), EF, and PA treatment did not decrease MΦ survival at any of the tested time points (data not shown). Additionally, protein levels were measured in MΦs treated with EdTx for 0, 2, 6, and 24 h. Protein levels did not change despite exposure to EdTx, further verifying that cell viability was not altered and thus allowing subsequent investigation of MΦ functions without having to correct for a reduction in the cell number over time (data not shown).

EdTx reduces the phagocytic capacity of human MΦs. When encountering microorganisms, MΦs undergo a rapid course of action consisting of chemotaxis, phagocytosis, and intracellular killing via oxygen-independent and oxygen-dependent (oxidative burst) mechanisms. Consequently, the effect of EdTx on MΦ phagocytosis of virulent *B. anthracis* Ames spores was investigated. Primary alveolar-like and HL-60 MΦs were pretreated with EdTx for 2, 6, or 24 h before being cocultured with spores at an MOI of 5 for 1 h. Control wells were left untreated, while other wells were treated with cytochalasin B before the addition of spores. This agent is a fungal toxin that disrupts actin filaments and was used as a positive control in this experiment and others in this study. All MΦs were then lysed and plated to quantify the number of organisms successfully phagocytosed in each well.

Figure 2 shows that the uptake of spores by both MΦ types was significantly inhibited following 6 and 24 h of EdTx exposure. Toxin treatment for 24 h exhibited a level of phagocytosis inhibition similar to that elicited by cytochalasin B treatment. Furthermore, MΦ phagocytosis of FITC-labeled *E. coli*-conjugated particles following EdTx treatment was analyzed. Similar to the spore uptake results, EdTx pretreatment for 3, 6, and 24 h significantly lowered human primary and HL-60 MΦ

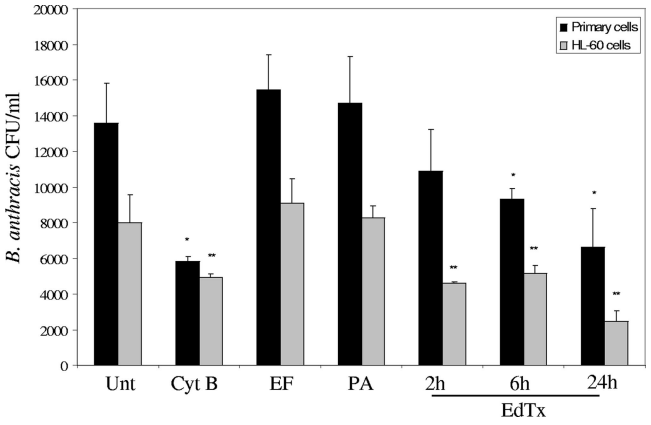

FIG. 2. EdTx pretreatment reduces uptake of *B. anthracis* Ames spores by human MΦs. Primary alveolar-like and HL-60 MΦs (5×10^5/well) were seeded in triplicate and pretreated with EdTx (1.25 μg/ml EF plus 5 μg/ml PA), EF (1.25 μg/ml), or PA (5 μg/ml) for 2 to 24 h. The cells were then infected with Ames spores (MOI = 5) for 1 h. Following gentamicin treatment and PBS washes, the cells were lysed and plated on blood agar plates. The colonies were counted, and the graph shows the combined results of three separate experiments performed with triplicate cultures ± standard deviations. *, $P < 0.05$ versus untreated primary cells; **, $P < 0.05$ versus untreated HL-60 cells (using ANOVA and Dunnett's tests).

phagocytosis of the *E. coli* particles (Fig. 3). To verify that LPS contamination from the purified toxin components was not responsible for this impaired phagocytosis, LPS (ranging from 1 to 100 ng/ml) was added to some wells for 24 h before exposure to the *E. coli* particles. However, phagocytosis was not altered post-LPS exposure, verifying that the impaired response was a result of EdTx itself. Only the 100-ng/ml group is shown in Fig. 3.

To explain the mechanism responsible for the decreased phagocytosis (as described above) exhibited by MΦs, it was hypothesized that two cAMP-binding signaling molecules, PKA and Epac, would likely be targeted by EdTx-generated cAMP. Therefore, cAMP analogs with specificity in their activation toward Epac or PKA were included to determine if stimulation of one or both pathways would mimic the results observed in response to EdTx treatment. 6-Bnz-cAMP is an activator of PKA, while 8-CPT-2Me is a selective Epac activator. Initially, a range of concentrations of these activators were chosen based on previous reports in the literature (8, 11, 28), and the effectiveness of compounds at these concentrations and their specificities for the respective molecules were verified with HL-60 MΦs (Fig. 4).

As expected, 6-Bnz-cAMP at all tested concentrations significantly enhanced PKA activity compared to untreated MΦs (Fig. 4A). Importantly, the Epac-selective analog 8-CPT-2Me did not alter PKA activity. We also treated cells with a highly specific myristoylated peptide PKA inhibitor, $mPKI_{14-22}$ (mPKI). As noted in Fig. 4A, mPKI treatment severely inhibited PKA activity. Because 300 μM 6-Bnz-cAMP activated PKA to a much greater extent than concentrations of 30 and 100 μM, we chose the 300 μM concentration for subsequent experiments.

To test the effectiveness and specificity of 8-CPT-2Me, Epac activation was assessed via a pull-down assay that examined its downstream target, Rap1. Treatment of HL-60 MΦs with 8-CPT-2Me increased levels of GTP-bound Rap1, indicating Epac activation, while 6-Bnz-cAMP had no effect on GTP-Rap1 expression (Fig. 4B). We noted that HL-60 MΦs treated

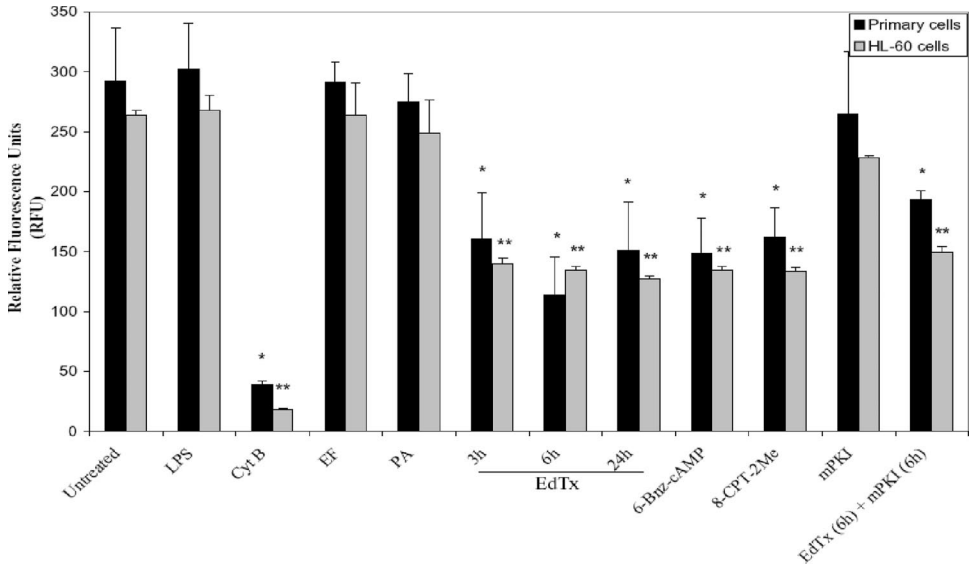

FIG. 3. Phagocytosis of FITC-conjugated *E. coli* particles by human MΦs is reduced after EdTx treatment. Primary alveolar-like and HL-60 MΦs (1×10^5/well) were seeded in quadruplicate and exposed to EdTx (1.25 μg/ml EF plus 5 μg/ml PA), EF (1.25 μg/ml), PA (5 μg/ml), cytochalasin B (10 μg/ml), LPS (100 ng/ml), or the cAMP analogs alone (300 μM 6-Bnz-cAMP, 25 μM mPKI, and 100 μM 8-CPT-2Me). One group received a combination of EdTx plus the PKA inhibitor mPKI for 6 h [EdTx (6h) + mPKI(6h)]. An aliquot (100 μl) of FITC-conjugated *E. coli* particles was then added for 1 h, and the fluorescence was measured. *, $P < 0.05$ versus untreated primary cells; **, $P < 0.05$ versus untreated HL-60 cells (using ANOVA and Dunnett's tests). One representative experiment of three is shown. The data are expressed as the mean plus standard deviation of the replicates.

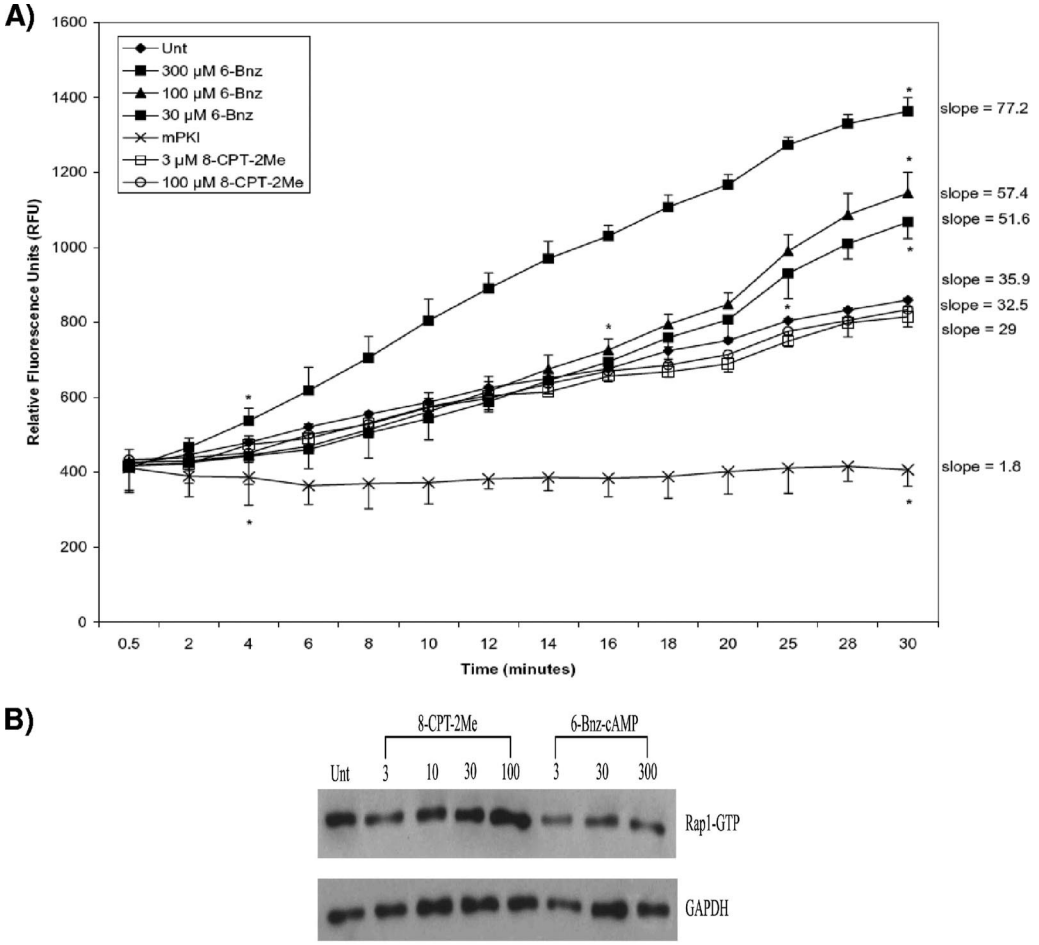

FIG. 4. Verifying the effectiveness and specificities of the cAMP analogs. Following treatment with various concentrations of 6-Bnz-cAMP, 8-CPT-2Me, or mPKI, HL-60 MΦs were lysed. (A) Samples (1 μg total protein each) were incubated with appropriate buffers, ATP, PKA substrate, and non-PKA inhibitor cocktail, and the fluorescence was collected every 2 min for 30 min. One representative graph of three independent experiments is shown. Asterisks mark the beginning and end of significance for each curve ($P < 0.05$ as determined by ANOVA and Dunnett's tests). The slope of each curve is also shown. The data are expressed as the mean ± standard deviation of the replicates. (B) Lysates were incubated with the GST fusion protein RBD of RalGDS immobilized to glutathione beads to specifically pull down the GTP-bound forms of Rap1. Next, samples were subjected to Western blot analysis using an anti-Rap1 primary antibody and an HRP-conjugated anti-rabbit secondary antibody. After being stained, the membranes were incubated in a chemiluminescence reagent and immediately exposed to X-ray film. The membranes were also immunoblotted with an HRP-GAPDH antibody to verify equal protein loading among lanes.

with a 100 μM concentration of 8-CPT-2Me activated Epac to a greater degree than the 3 and 30 μM concentrations. Consequently, in our later experiments, we used a 100 μM concentration of this Epac activator.

Similar to the EdTx groups, 6-Bnz-cAMP and 8-CPT-2Me significantly suppressed the phagocytic uptake of *E. coli* particles by primary alveolar-like and HL-60 MΦs (Fig. 3). Because PKA and Epac activation mimicked the EdTx-induced inhibition of uptake, it suggested that both pathways were potentially involved in the effects elicited by EdTx. As shown in Fig. 3, mPKI did not cause phagocytosis inhibition like that elicited by EdTx. A final group was exposed to EdTx and mPKI simultaneously for 6 h in order to prevent potential PKA activation by EdTx. In both MΦ cell types, phagocytosis was still reduced, suggesting this was not a process solely dependent on PKA. Because EdTx elicited similar levels of impairment of phagocytosis in both the primary and immortalized HL-60 MΦs, the latter cell type was determined to be a suitable model of primary human MΦs and was used in all subsequent experiments.

Since it appeared that both the PKA and Epac pathways might be responsible for the observed phagocytosis impairment in EdTx-treated human MΦs, we next verified that the concentration of the cAMP analogs utilized in Fig. 3 was not so high that it might have possibly masked any differential effects between the two signaling molecules. Therefore, the concentration dependence of the two analogs in regard to phagocytosis inhibition was then tested (Fig. 5). For this experiment, HL-60 MΦs were treated with the indicated concentrations of 6-Bnz-cAMP, 8-CPT-2Me, or a combination of the two before phagocytic uptake of FITC-labeled *E. coli* Bioparticles was assessed. As Fig. 5 shows, even 100 to 200 μM concentrations of 6-Bnz-cAMP and 30 to 100 μM 8-CPT-2Me significantly impaired phagocytosis. Further, phagocytosis was also significantly lowered when 100 to 300 μM of 6-Bnz-cAMP and 30 to

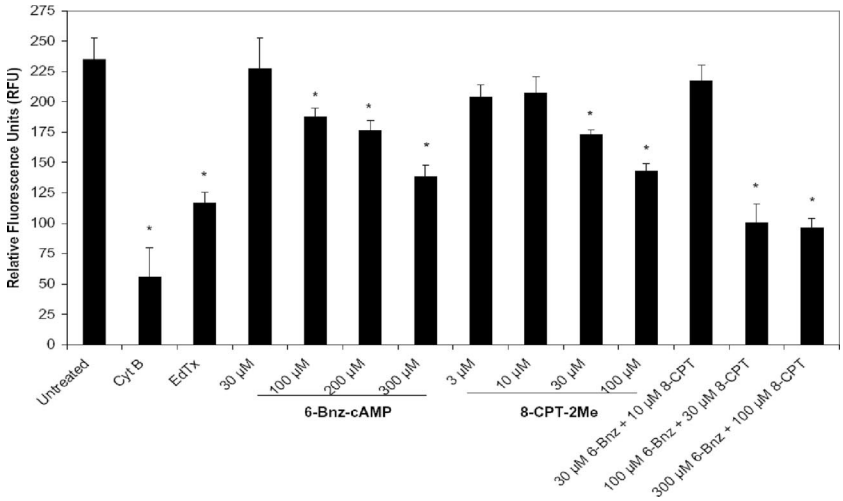

FIG. 5. Examining the effect of the cAMP analog concentration on phagocytosis. HL-60 MΦs (1×10^5/well) were seeded in quadruplicate and pretreated for 1 h with the indicated concentrations of the cAMP analogs, cytochalasin B (10 μg/ml), or EdTx (1.25 μg/ml EF plus 5 μg/ml PA for 24 h). FITC-conjugated Bioparticles were then added for 1 h, and the intracellular fluorescence was measured. *, $P < 0.05$ versus untreated cells (ANOVA and Dunnett's tests). One representative experiment of three is shown. The data are expressed as the means ± standard deviations for the quadruplicate wells.

100 μM of 8-CPT-2Me were tested in combination (Fig. 5). Uptake of *E. coli* Bioparticles did not appear to be lessened at 30 μM 6-Bnz-cAMP and 3 to 10 μM 8-CPT-2Me. Likewise, activation of their respective molecules (PKA and Epac) at these low concentrations of 6-Bnz-cAMP and 8-CPT-2Me was not as enhanced as that achieved by the higher concentrations of analogs (Fig. 4B). Thus, we continued using the 300 μM 6-Bnz-cAMP and 100 μM 8-CPT-2Me doses for subsequent experiments because they activated PKA or Epac to the greatest degree while providing a level of phagocytosis suppression similar to that caused by EdTx.

Overall, these experiments indicated that EdTx impaired human MΦ phagocytosis. Application of selective PKA and Epac activators caused a similar reduction in phagocytosis, implicating both of the pathways as potential mediators in EdTx-induced cAMP signaling. The suppressed phagocytosis, together with the previously reported impairment in MΦ migration following EdTx treatment (56), raised the possibility that the actin cytoskeleton was involved.

Treatment with EdTx reduces MΦ cytoskeletal spreading and F-actin levels. To examine the possibility of EdTx-induced cytoskeletal changes, the effect on MΦ cell spreading was next examined. MΦs were exposed to EdTx for 2, 6, 12, and 24 h. FITC-labeled *E. coli* particles were then added for 1 h to stimulate cellular movement. Following staining with phalloidin, a fluorescence microscope was used to view and capture images of cells under each condition. In the untreated group exposed to the *E. coli* particles, the majority of MΦs displayed a spread-out morphology with numerous actin-rich membrane protrusions called filopodia (Fig. 6A). EdTx treatment for 6 and 24 h caused reorganization of the actin cytoskeleton so that the cells appeared less spread out and displayed a reduced number of filopodia (Fig. 6C and D). Cytochalasin B also altered the morphology of the cells and reduced the number of filopodia, as shown in Fig. 6B. Manually tracing the footprints of the cells with ImageJ software (see Materials and Methods) allowed calculation of the mean cellular area (Fig. 6E), which was then converted to the spreading index. The spreading index of toxin-pretreated MΦs dropped significantly at 6, 12, and 24 h compared to untreated cells (spreading indexes of 0.8, 0.6, and 0.6, respectively, compared to an untreated-cell index of 1). The cell elongation index, defined as the length/width ratio, did not change among the groups (data not shown).

Similarly, the F-actin content of the MΦs was significantly lowered in response to EdTx treatment, as determined by an immunofluorescence assay that labeled actin with phalloidin. Cells were treated with toxin for 2, 6, and 24 h before being cultured with FITC-labeled *E. coli*-conjugated particles and labeled with phalloidin. The cells pretreated for 6 and 24 h with EdTx contained approximately 1.6-fold less F-actin than untreated cells (Fig. 7). This was almost as great a reduction in F-actin levels as that evoked by the positive control, cytochalasin B (a 1.7-fold drop). Treating groups with 6-Bnz-cAMP and 8-CPT-2Me (Fig. 7) revealed that activating both the PKA and Epac pathways mimicked the EdTx-induced effects. Inhibiting PKA with mPKI did not have an effect on F-actin levels compared to those in untreated cells. Similar to results in the phagocytosis experiment, wells that received a combination of PKA inhibitor and EdTx simultaneously showed reduced F-actin content. Because the actin reduction was still seen, even when PKA was not allowed to become activated (the inhibitory activity of mPKI is shown in Fig. 4A), it implied that another pathway, in addition to PKA, was involved.

Together, these experiments indicated that EdTx interfered with cytoskeletal rearrangements, as detected by inhibition of the cell-spreading response, reduced filopodia, and lowering of F-actin content. The results also provided further evidence to support a role for both pathways (PKA and Epac) in downstream EdTx-generated cAMP signaling.

MΦ PKA/Epac-1 protein levels and activity are altered following EdTx treatment. Due to the targeting of the PKA and Epac pathways by EdTx-generated cAMP in MΦs, the effect of

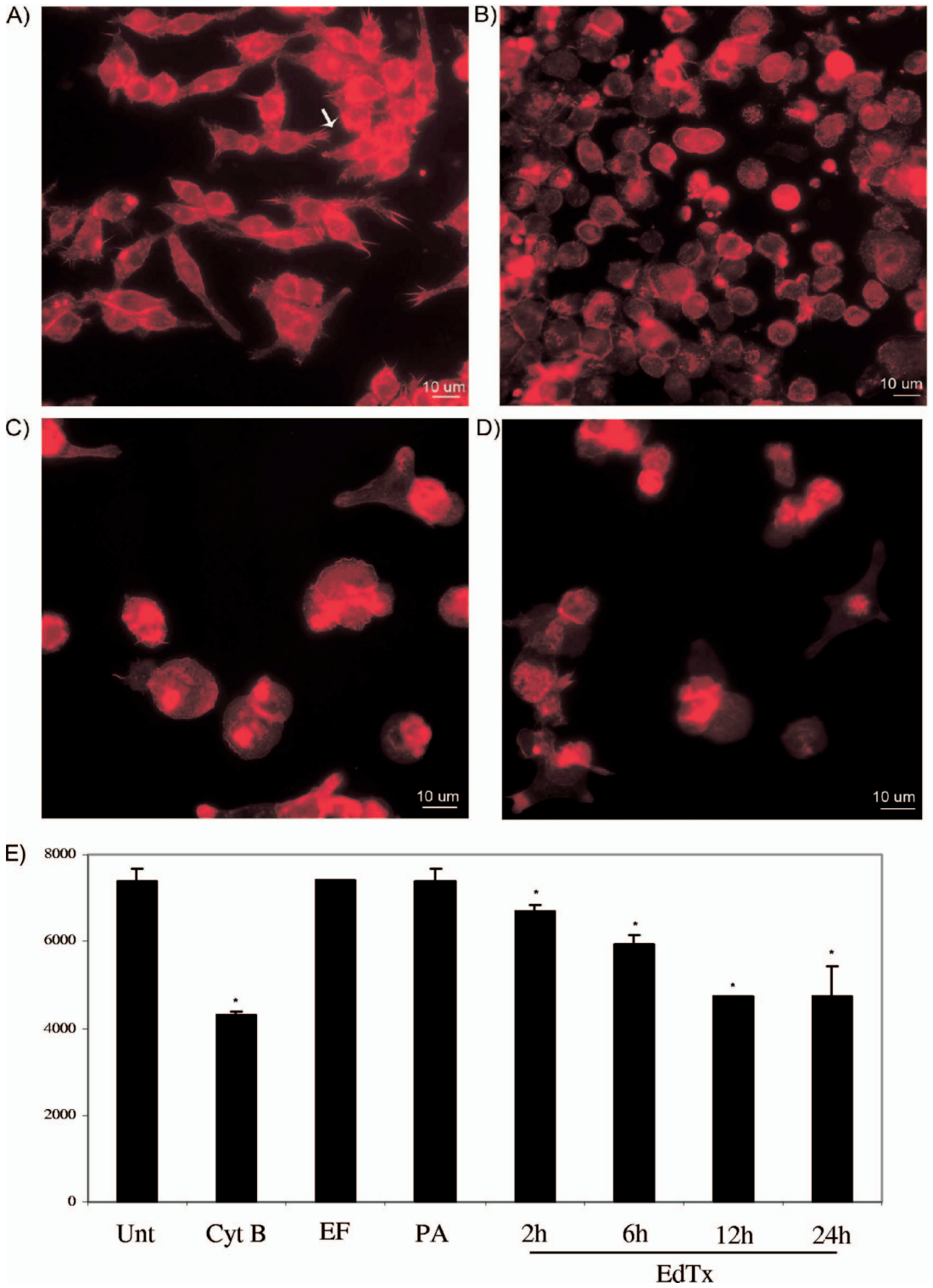

FIG. 6. The morphological responses and spreading index of EdTx-treated MΦs differ from those of untreated cells. HL-60 MΦs on glass coverslips were treated with EdTx (1.25 μg/ml EF plus 5 μg/ml PA), cytochalasin B, EF alone (1.25 μg/ml), or PA alone (5 μg/ml) (not shown) for various times. FITC-labeled *E. coli* particles were added for 1 h, and then the cells were permeabilized, fixed, and stained with phalloidin. (A) Untreated cells (the arrow points to filopodia). (B) Cells treated with cytochalasin B for 2 h. (C) Six-hour EdTx treatment. (D) Twenty-four-hour EdTx treatment. (E) Images containing at least 100 randomly selected cells in five fields of view were captured, and ImageJ software was used to calculate the area of each cell. The graph shows the combined results of three independent experiments carried out on duplicate wells ± standard deviations. The asterisks indicate statistical significance ($P < 0.05$) using ANOVA and the Student-Newman-Keub method.

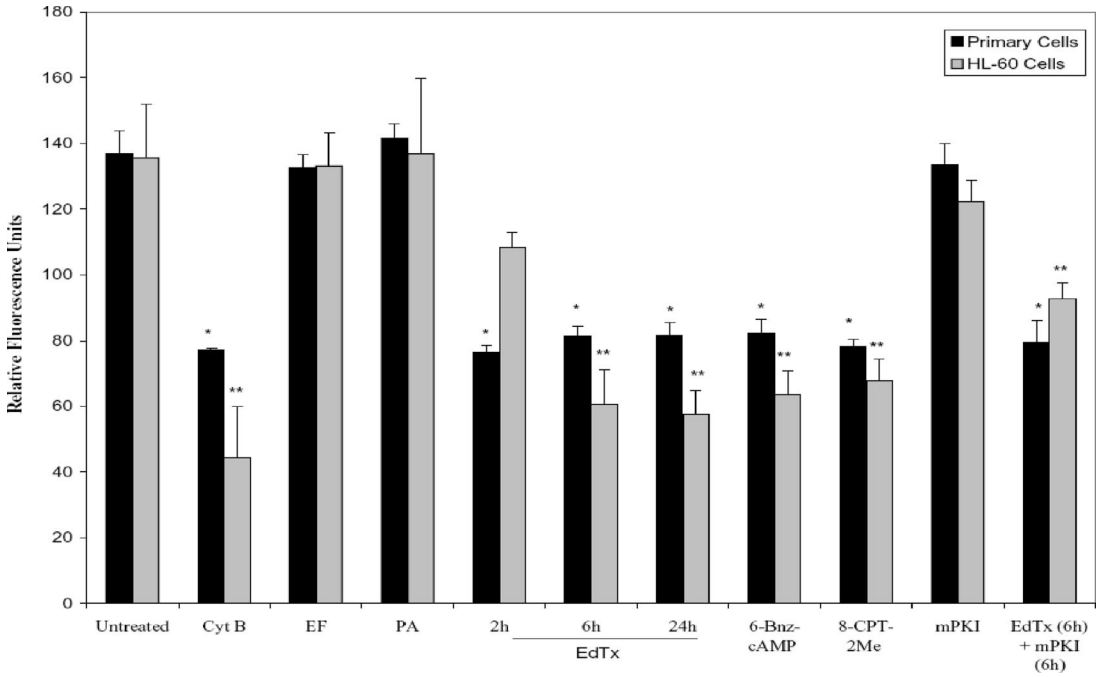

FIG. 7. EdTx treatment reduces the F-actin content of human MΦs. Primary alveolar-like and HL-60 MΦs (2.5×10^5/well) in 96-well plates were pretreated with EdTx (1.25 μg/ml EF plus 5 μg/ml PA), EF (1.25 μg/ml), PA (5 μg/ml), or cytochalasin B (10 μg/ml). Some groups were pretreated with 6-Bnz-cAMP (PKA activator; 300 μM), mPKI (PKA inhibitor; 25 μM), or 8-CPT-2Me (Epac activator; 100 μM) alone for 1 h. Additionally, one treatment group received a combination of EdTx and mPKI for 6 h [EdTx (6h) + mPKI (6h)]. FITC-labeled *E. coli*-conjugated particles were added for 1 h to provide phagocytic stimuli. The cells were then fixed, permeabilized, and actin labeled with Alexa Fluor-conjugated phalloidin. Fluorescence was measured with a plate reader, and the graph shows the results of one of three repeats. *, $P < 0.05$ versus untreated primary cells; **, $P < 0.05$ versus untreated HL-60 cells (using ANOVA and Dunnett's tests). The data are expressed as the means ± standard deviations for the quadruplicate wells.

EdTx on the production of the two molecules was next examined. Western blot analysis of PKA protein levels in toxin-treated MΦ lysates revealed a time-dependent alteration of the regulatory type II subunit of PKA (RIIα). Compared to untreated MΦs, PKA RIIα levels initially increased after a 2-h treatment but then dropped below normal levels after a 6- to 24-h toxin exposure (Fig. 8A). Contrary to the depressed expression of PKA RIIα observed at time points beyond 2 h, Epac-1 showed increased production at all tested time points. Protein levels were enhanced between 2.4- and 3.4-fold after 2 to 24 h of toxin treatment (Fig. 8B). These data indicated that MΦs were responding to the increased cAMP production induced by EdTx by altering production of the two signaling proteins that directly bound cAMP molecules.

Because PKA RIIα levels were altered during the toxin treatment time course, the enzymatic activity of PKA as a whole was evaluated with a fluorescence-based kinase assay. Similar to the protein production results, the 1- and 2-h EdTx treatment significantly increased PKA activity compared to untreated cells (Fig. 9). However, the 6-h pretreatment resulted in activity very similar to that of untreated control cells, and PKA activity among the 24-h samples was significantly lower than among samples of the untreated group.

To address the effect of EdTx on Epac-1 activity in HL-60 MΦs, the activity of Rap1, the small GTPase directly activated by Epac-1, was used as an indicator of Epac activation. Detection of GTP-bound Rap1 after toxin treatment times of 2, 6, and 24 h was evaluated. As Fig. 10 shows, GTP-Rap1 levels were increased (approximately two- to threefold) compared to that for untreated cell lysate, and the levels remained elevated even 24 h post-toxin treatment.

DISCUSSION

EdTx is one of several powerful weapons utilized by *B. anthracis* to thwart host immune defenses and establish a successful infection. It belongs to the same class of adenylate cyclases as Exo Y of *Pseudomonas aeruginosa*, adenylate cyclase of *Yersinia pestis*, and adenylate cyclase toxin of *Bordetella pertussis* (reviewed in reference 3). The intrinsic adenylate cyclase activity of EdTx upsets the delicate physiological equilibrium inside a wide variety of cells. For years, it was speculated that this would lead to a suppressed immune response, but only recently has this prospect started to be explored. It is now known that EdTx disrupts cytokine networks in monocytes (29), inhibits platelet aggregation (6), reduces MΦ and T-cell migration (56), and disrupts T-cell functions (16, 51), to list just a few examples.

The MΦ actin cytoskeleton is a highly dynamic structure that rapidly adapts to the cells' demands in order to successfully utilize two of its powerful weapons: motility and phagocytosis. Each of these processes is highly complex, but continuous feedback from the extracellular milieu and surrounding cells allows the MΦ to be a quick responder during a microbial invasion. During *B. anthracis* infection, human monocytes and murine MΦs are subject to the adenylate cyclase activity of

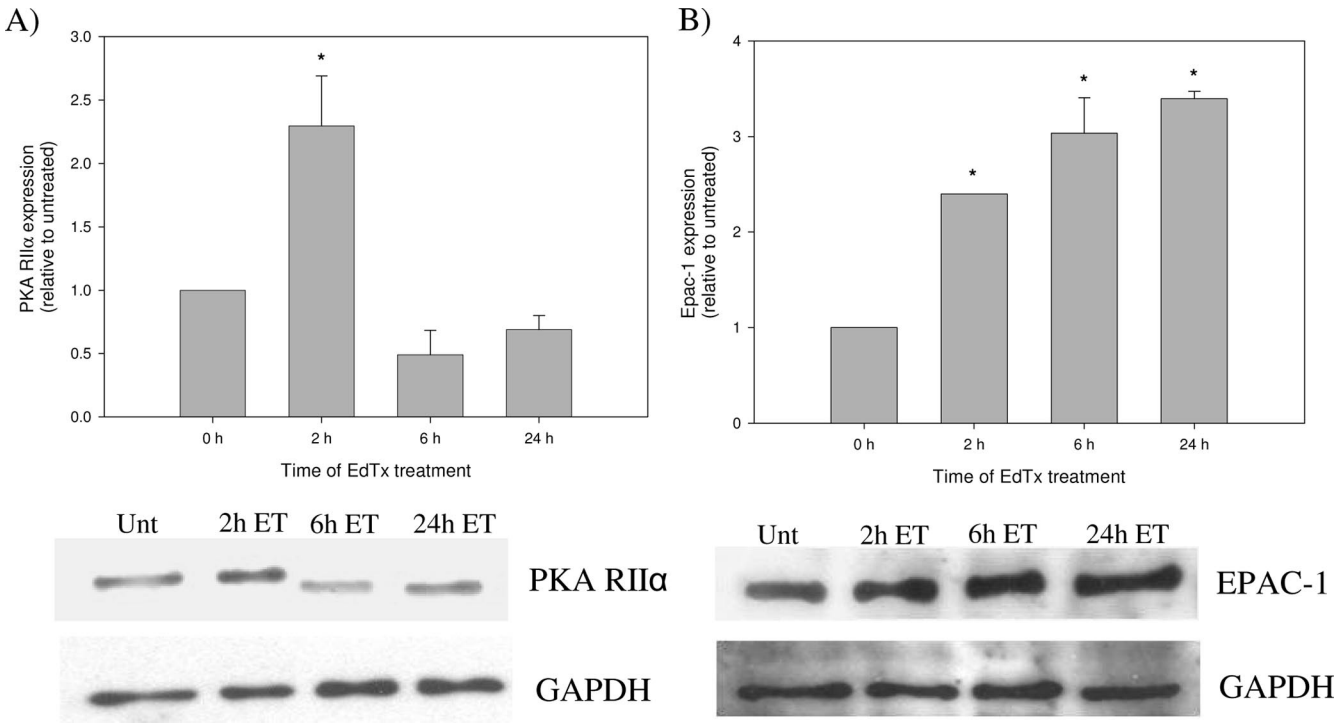

FIG. 8. EdTx alters the expression of PKA RIIα and Epac. Following toxin treatment (1.25 μg/ml EF plus 5 μg/ml PA), HL-60 MΦs were lysed and samples were subjected to Western blot analysis with antibodies against PKA RIIα (A) and Epac-1 (B). Densitometry was performed for each band, and the data are expressed as the change compared to untreated control cells. The experiment was performed independently three times, and the graphs depict the averages from all three experiments performed with duplicate cultures ± standard deviations. Below each graph is an image of the Western blot against PKA RIIα (A) and Epac-1 (B), along with the results of blotting against GAPDH to verify equal protein loading. *, $P < 0.05$ by ANOVA and Dunn's test.

EdTx (29, 41). As predicted, EdTx generated a strong surge of cAMP in the human HL-60 and primary MΦs in a dose- and time-dependent manner. For instance, after a 6-h exposure of HL-60 cells to EdTx, combined intracellular and extracellular cAMP levels were 38-fold greater than in untreated HL-60 MΦs. We assessed intracellular levels of cAMP because some signaling can result from the intracellular pool; however, we also examined extracellular levels because cAMP can diffuse into neighboring cells and modulate their effects.

The levels of cAMP secreted by EdTx-treated HL-60 MΦs were much higher than those produced by EdTx-treated primary MΦs. This might be due to the differing methods of MΦ differentiation used to prepare the two cell types (PMA treatment versus GM-CSF). Also, the amount of cAMP evoked by EdTx appeared to be highly dependent upon the cell type. For example, human neutrophils and RAW 264.7 murine MΦs were not particularly sensitive to EdTx, while Chinese hamster ovary (CHO) cells and human lymphocytes were extremely sensitive (41). It was demonstrated that injecting mice intravenously with EdTx resulted in organ lesions and the death of the animals (23). Although we could not directly compare the toxin doses administered in vivo (100 μg EF plus 100 μg PA) with the concentration used in these in vitro experiments (1.25 μg/ml EF plus 5 μg/ml PA), it is important to note that neither the primary nor the HL-60 MΦs were susceptible to killing following exposure to EdTx. It appeared that cells varied in their susceptibility to EdTx-induced lethality, as CHO cells were not killed by the toxin, while RAW 264.7 murine MΦs were susceptible to the effect of the toxin (61).

The ability of EdTx, as well as LeTx, to inhibit migration of human MΦs by downregulating chemokine receptor signaling was recently discovered (56). However, the effect of EdTx on MΦ phagocytosis remained unknown. Our study is the first to report the ability of EdTx to reduce the phagocytosis of both virulent Ames spores and *E. coli* particles by human primary cells and a human cell line. Uptake inhibition was observed after all toxin pretreatment times, ranging from 3 to 24 h. The reduction in phagocytosis was not an artifact due to depletion of the MΦ population, as MΦ survival was not affected by EdTx exposure. Although MΦs are considered a favorable site for spore germination and a mechanism of transportation to the lymph nodes, it has been shown that MΦs kill the majority of intracellular spores and vegetative cells (32, 35, 62). These data also correlated with our observation that human monoclonal antibody to PA blocked dissemination of *B. anthracis* Ames spores to the bloodstream from the lungs (52).

The ability of EdTx to reduce the likelihood of spore/bacillus phagocytosis by MΦs is likely important during later stages of infection, particularly when large volumes of EdTx are being secreted by rapidly multiplying extracellular vegetative cells. At this time, EdTx-induced suppression of MΦ phagocytosis would be of tremendous benefit to the survival of the bacteria and any viable dormant spores and would likely increase the host's susceptibility to fulminant anthrax disease. Similar to

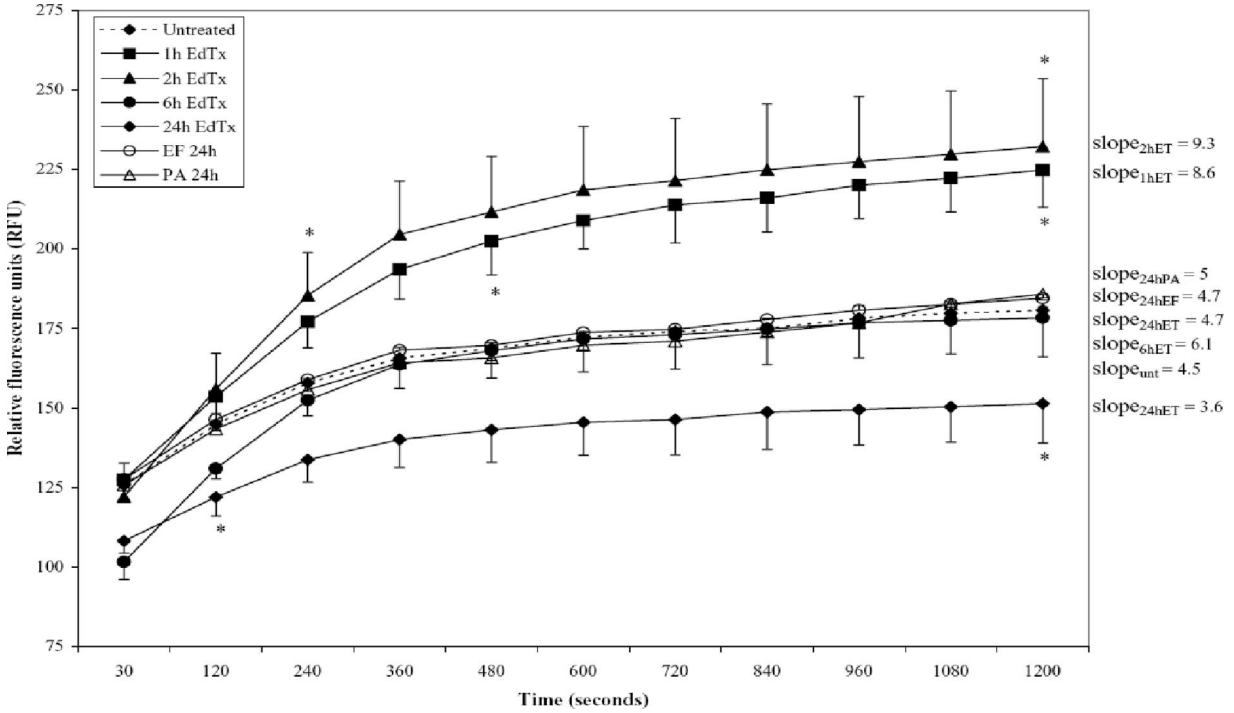

FIG. 9. PKA activity is altered by EdTx in a time-dependent manner. Following EdTx treatment (1.25 μg/ml EF plus 5 μg/ml PA), HL-60 MΦs were lysed. Samples (1 μg total protein each) were then incubated with appropriate buffers, ATP, PKA substrate, and non-PKA inhibitor cocktail, and fluorescence was collected every 2 min for 20 min. Controls consisting of EF (1.25 μg/ml) and PA (5 μg/ml) alone did not influence PKA activity. One representative graph of three independent experiments is shown. The asterisks mark the beginning and end of significance for each curve ($P < 0.05$ as determined by ANOVA and Dunnett's tests). The slope for each curve is also shown. The data are expressed as the mean ± standard deviation of the replicates.

our findings, a previous publication showed that EdTx-treated human neutrophils exhibited impaired uptake of Sterne spores (50). Thus, the ability of EdTx to lower phagocytic uptake by two types of the host's professional phagocytes, MΦs and neutrophils, may explain how quickly the organism begins to multiply systemically and infiltrate numerous host tissues.

To explain the lowered phagocytic activity, we hypothesized that impairment of the actin cytoskeleton may be a downstream effect elicited by such high production of EdTx-generated cAMP. Indeed, our studies demonstrated that EdTx treatment brought about morphological changes in the actin cytoskeleton of HL-60 MΦs. Cells contained fewer filopodia than untreated cells, even in the presence of FITC-conjugated *E. coli* particles, and although the cytoskeleton appeared intact and complete, EdTx exposure reduced the cell spreading index of MΦs in a time-dependent manner. Formation of pseudopodia and filopodia during phagocytosis requires actin nucleation, which is formation of new actin filaments, along with an increase in the length of existing filaments (47). Along with the reduced filopodium response observed in this study, the F-actin contents of both MΦ types were also significantly impaired as early as 6 h post-toxin treatment, and the impairment was sustained even at 24 h.

The observed defects in actin rearrangement and F-actin content were supported and possibly explained by the striking downregulation of multiple genes related to the cytoskeleton that was published previously by our laboratory (17). Microarray analysis revealed, for instance, that the gene encoding PDZ and LIM domain protein 2 (PDLIM2) was downregulated 6.8-fold in murine MΦs after 6 h of EdTx treatment. This adaptor protein, located on the actin cytoskeleton, promotes cell attachment by interacting with extracellular matrix proteins (45). Formin-binding protein-1 like (FNBP1L) is a microtubule-associated protein that is predicted to function as a scaffolding protein for microtubules, Rho family GTPases, and WASP family proteins (37). FNBP1L can also promote actin nucleation (27), and the gene encoding the protein was downregulated 8.9-fold in EdTx-treated RAW 264.7 cells. Additionally, switch-associated protein 70 (SWAP-70) interacts with Rac and mediates signaling leading to membrane ruffling (58). This protein can also bind F-actin directly, and mutant cells exhibited abnormal actin rearrangement and migration deficiencies (34). The gene for SWAP-70 was downregulated 3.6-fold post-toxin treatment (17).

Due to their abilities to directly bind cAMP and participate in cAMP signaling cascades, we determined whether the PKA pathway alone, the Epac pathway alone, or a combination of the two pathways was responsible for translating the large accumulation of intracellular cAMP into the altered MΦ phenotypes and inhibited functions described in this study. MΦs treated with EdTx for 2 h exhibited increased expression of PKA RIIα, corresponding to the beginning of the increase in intracellular cAMP caused by the adenylate cyclase activity of EdTx. This early time point of toxin treatment also led to significantly greater PKA activity than samples collected from untreated MΦs. PKA activation at 2 h was previously observed

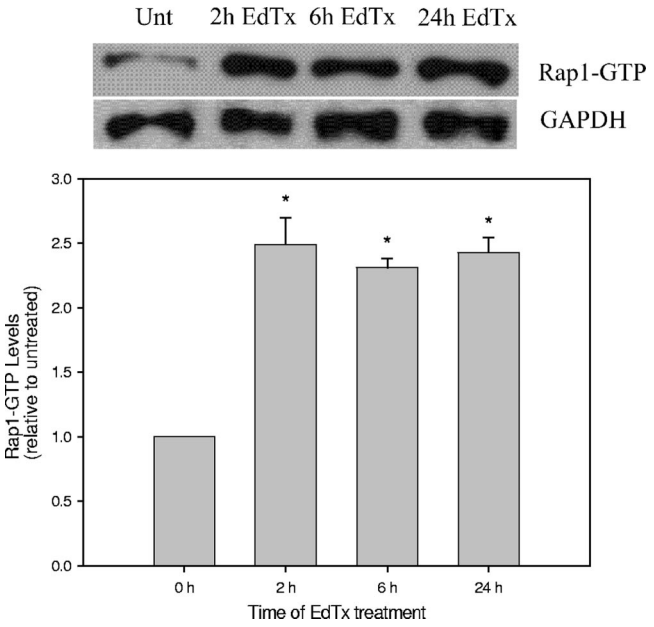

FIG. 10. Epac activation of Rap1 is enhanced by EdTx. Following EdTx treatment (1.25 μg/ml EF plus 5 μg/ml PA), HL-60 MΦs were lysed. The lysates were incubated with GST-RalGDS-RBD immobilized to glutathione beads to specifically pull down the GTP-bound forms of Rap1. Next, samples were subjected to Western blot analysis using an anti-Rap1 primary antibody and an HRP-conjugated anti-rabbit secondary antibody. The membranes were also immunoblotted with an HRP-GAPDH antibody to verify equal protein loading among lanes. Below the image is a graph of densitometry that was performed for each band, and the data are expressed as the change compared to untreated control cells. The experiment was performed independently two times, and the graph shows the averages from the experiments carried out with duplicate cultures ± standard deviations. *, $P < 0.05$ by ANOVA and Dunn's test.

in EdTx-treated rabbit platelets (6). After 6 to 24 h of EdTx treatment, however, PKA RIIα expression levels were downregulated. These data corresponded to time points when cAMP levels were significantly higher in toxin-treated cells versus untreated cells. Similar to the protein expression trends, it was determined that at 6 h, EdTx-treated MΦs showed a PKA activity curve very similar to that of untreated cells, and the 24-h toxin treatment produced an activity curve significantly lower than that of untreated MΦs. Downregulation of the regulatory subunit of PKA, which contains cAMP-binding sites, at the later time points, as well as impaired PKA activity, may represent the target cell's strategy to compensate for the flood of cAMP produced by EdTx and an attempt to return the cell to a basal state.

Epac-1 protein levels, on the other hand, remained elevated throughout the time course of toxin exposure. The activity pattern of Epac, assessed by examining levels of activated Rap1, also resembled the expression data, as the amount of GTP-bound Rap1 became elevated 2 h post-toxin exposure and remained high for as long as 24 h. Because the effects of EdTx on MΦ function were stronger at 6 h and beyond, when PKA expression/activity were downregulated and Epac expression/activity were upregulated, perhaps Epac is principally responsible for the effects of EdTx at the later time points. It was next considered that the disruption in the balance of PKA/Epac protein production and activity initiated by EdTx was ultimately responsible for the reduced phagocytosis, F-actin content, and cell spreading observed in toxin-treated cells.

Phosphodiesterase-resistant cAMP analogs that are highly specific in their activation of either PKA or Epac have been developed in recent years (14). We incorporated the best characterized of these compounds (6-Bnz-cAMP, mPKI, and 8-CPT-2Me) to determine which pathway the EdTx-generated cAMP targeted to in order to cause the observed inhibition of phagocytosis and cell spreading.

Pretreatment of cells with 6-Bnz-cAMP and 8-CPT-2Me, activators of PKA and Epac, respectively, during phagocytosis of FITC-conjugated *E. coli* particles resulted in inhibition of uptake by both types of MΦs. The inhibition mimicked the conditions of toxin-treated cells, suggesting that EdTx-generated cAMP likely targeted both the PKA and Epac-1 pathways in order to cause such a decline in phagocytosis. These results were in agreement with a previous report showing that activation of the PKA and Epac pathways was capable of reducing the phagocytic activity of human monocyte-derived MΦs (11) and rat alveolar MΦs (8).

These compounds were also included in the F-actin content experiments. Similar to the phagocytosis experiments, pretreatment with 6-Bnz-cAMP revealed that activation of PKA was likely involved in EdTx-related events. An additional treatment group suggested that another pathway was participating in the cAMP signaling events, and pretreatment with 8-CPT-2Me implicated the Epac-1 pathway as a likely candidate. Experiments involving short interfering RNA approaches with PKA and Epac are currently under way in our laboratory to provide further evidence of the roles of the two molecules following EdTx treatment. It is important to note that although PKA and Epac seem to play major roles with regard to EdTx signaling in MΦs, participation by other signaling proteins cannot be excluded.

Though they were once believed to play only a moderate role during anthrax infection, mounting evidence of sporicidal and bactericidal behavior exhibited by MΦs is shifting this view (13, 35, 62). Mice depleted of MΦs before challenge with Ames spores were more susceptible to infection and exhibited higher bacterial loads than saline-treated mice (18). Although it was once only speculated, it has become clear, through this study and others, that the high quantity of cAMP produced by the intrinsic adenylate cyclase nature of EdTx does indeed allow it to disrupt key functions of MΦs, thus crippling an important arm of the host's innate immune system. In addition to EdTx impairing MΦ chemotaxis (56) and disturbing monocyte cytokine signaling (29), the decrease of the phagocytic activity and cell-spreading response of human MΦs through targeting of the PKA and Epac pathways provides further evidence of the powerful activity of EdTx.

ACKNOWLEDGMENT

This study was supported in part by the NIAID (N01-AI-30065).

REFERENCES

1. **Abrami, L., M. Fivaz, and F. van der Goot.** 2000. Adventures of a pore-forming toxin at the target cell surface. Trends Microbiol. **8:**168–172.
2. **Abrami, L., N. Reig, and F. van der Goot.** 2005. Anthrax toxin: the long and winding road that leads to the kill. Trends Microbiol. **13:**72–78.
3. **Ahuja, N., P. Kumar, and R. Bhatnagar.** 2004. The adenylate cyclase toxins. Crit. Rev. Microbiol. **30:**187–196.

4. **Akagawa, K.** 1994. Differentiation and function of human monocytes. Hum. Cell **7:**116–120.
5. **Akagawa, K.** 2002. Functional heterogeneity of colony-stimulating factor-induced human monocyte-derived macrophages. Int. J. Hematol. **76:**27–34.
6. **Alam, S., M. Gupta, and R. Bhatnagar.** 2005. Inhibition of platelet aggregation by anthrax edema toxin. Biochem. Biophy. Res. Commun. **339:**107–114.
7. **Andressen, R., W. Brugger, C. Scheibenbogen, M. Kreutz, H. Leser, A. Rehm, and G. Lohr.** 1990. Surface phenotype analysis of human monocyte to macrophage maturation. J. Leukoc. Biol. **47:**490–497.
8. **Aronoff, D., C. Canetti, C. Serezani, M. Luo, and M. Peters-Golden.** 2005. Cutting edge: macrophage inhibition by cyclic AMP (cAMP): differential roles of protein kinase A and exchange protein directly activated by cAMP-1. J. Immunol. **174:**595–599.
9. **Ben Nasr, A., J. Haithcoat, J. Masterson, J. Gunn, T. Eaves-Pyles, and G. Klimpel.** 2007. Critical role for serum opsonins and complement receptors CR3 (CD11b/CD18) and CR4 (CD11c/CD18) in phagocytosis of *Francisella tularensis* by human dendritic cells (DC): uptake of *Francisella* leads to activation of immature DC and intracellular survival of the bacteria. J. Leukoc. Biol. **80:**774–786.
10. **Bradley, K., J. Mogridge, M. Mourez, R. Collier, and J. Young.** 2001. Identification of the cellular receptor for anthrax toxin. Nature **414:**225–229.
11. **Bryn, T., M. Mahic, J. Enserink, F. Schwedem, E. Aandahl, and K. Tasken.** 2006. The cyclic AMP-Epac1-Rap1 pathway is dissociated from regulation of effector functions in monocytes but acquires immunoregulatory function in mature macrophages. J. Immunol. **176:**7361–7370.
12. **Cantarow, W., H. Cheung, and G. Sundharads.** 1978. Effects of prostaglandins on the spreading, adhesion, and migration of mouse peritoneal macrophages. Prostaglandins **16:**39–42.
13. **Chakrabarty, K., W. Wu, J. Booth, E. Duggan, K. Coggeshall, and J. Metcalf.** 2006. *Bacillus anthracis* spores stimulate cytokine and chemokine innate immune responses in human alveolar macrophages through multiple mitogen-activated protein kinase pathways. Infect. Immun. **74:**4430–4438.
14. **Christensen, A., J. Selheim, S. de Rooj, F. Dremier, F. Schwede, K. Dao, A. Martinez, C. Maenhaut, J. Bos, H. Genieser, and S. Doskeland.** 2003. cAMP analog mapping of Epac1 and cAMP kinase: discriminating analogs demonstrate that Epac and cAMP kinase act synergistically to promote PC-12 cell neurite extension. J. Biol. Chem. **278:**35394–35402.
15. **Collins, S.** 1987. The HL-60 promyelocytic leukemia cell line: proliferation, differentiation, and cellular oncogene expression. Blood **70:**1233–1244.
16. **Comer, J., A. Chopra, J. Peterson, and R. Konig.** 2005. Direct inhibition of T-lymphocyte activation of anthrax toxins in vivo. Infect. Immun. **73:**8275–8281.
17. **Comer, J., C. Galindo, F. Zhang, A. Wenglikowski, K. Bush, H. Garner, J. Peterson, and A. Chopra.** 2006. Murine macrophage transcriptional and functional responses to *Bacillus anthracis* edema toxin. Microb. Pathog. **41:**96–110.
18. **Cote, C., N. Van Rooijen, and S. Welkos.** 2006. Roles of macrophages and neutrophils in the early host response to *Bacillus anthracis* spores in a mouse model of infection. Infect. Immun. **74:**469–480.
19. **Crawford, M., C. Aylott, R. Bourdeau, and G. Bokoch.** 2006. *Bacillus anthracis* toxins inhibit human neutrophil NADPH oxidase activity. J. Immunol. **176:**7557–7565.
20. **de Rooij, J., F. J. Zwartkruis, M. H. Verheijen, R. H. Cool, S. M. Nijman, A. Wittinghofer, and J. L. Bos.** 1998. Epac is a Rap1 guanine-nucleotide-exchange factor directly activated by cyclic AMP. Nature **396:**474–477.
21. **Dixon, T., M. Meselson, J. Guillemin, and P. Hanna.** 1999. Anthrax. N. Engl. J. Med. **341:**815–826.
22. **Drum, C. L., S. Z. Yan, J. Bard, Y. Q. Shen, D. Lu, S. Soelaiman, Z. Grabarek, A. Bohm, and W. J. Tang.** 2002. Structural basis for the activation of anthrax adenylyl cyclase exotoxin by calmodulin. Nature **415:**396–402.
23. **Firoved, A., G. Miller, M. Moayeri, R. Kakkar, Y. Shen, J. Wiggins, E. McNally, W. Tang, and S. Leppla.** 2005. *Bacillus anthracis* edema toxin causes extensive tissue lesions and rapid lethality in mice. Am. J. Pathol. **167:**1309–1320.
24. **Fontana, J., D. Colbert, and A. Deisseroth.** 1981. Identification of a population of bipotent stem cells in the HL60 human promyelocytic leukemia cell line. Proc. Natl. Acad. Sci. USA **78:**3863–3866.
25. **Friedlander, A.** 1999. Clinical aspects, diagnosis, and treatment of anthrax. J. Appl. Microbiol. **87:**303.
26. Reference deleted.
27. **Ho, H., R. Rohatgi, A. Lebensohn, L. Ma, J. Li, S. Gygi, and M. Kirschner.** 2004. Toca-1 mediates Cdc42-dependent actin nucleation by activating the N-WASP-WIP complex. Cell **118:**203–216.
28. **Hong, J., R. Doebele, M. Lingen, L. Quilliam, W. Tang, and M. Rosner.** 2007. Anthrax edema toxin inhibits endothelial cell chemotaxis via Epac and Rap1. J. Biol. Chem. **282:**19781–19787.
29. **Hoover, D., A. Friedlander, L. Rogers, and I. Yoon.** 1994. Anthrax edema toxin differentially regulates LPS-induced monocyte production of tumor necrosis factor alpha and interleukin-6 by increasing intracellular cAMP. Infect. Immun. **62:**4432–4439.
30. **Howe, A.** 2004. Regulation of actin-based cell migration by cAMP/PKA. Biochim. Biophys. Acta **1692:**159–174.
31. **Howe, A., L. Baldor, and B. Hogan.** 2005. Spatial regulation of the cAMP-dependent protein kinase during chemotactic cell migration. Proc. Natl. Acad. Sci. USA **102:**14320–14325.
32. **Hu, H., Q. Sa, T. Koehler, A. Aronson, and D. Zhou.** 2006. Inactivation of *Bacillus anthracis* spores in murine primary macrophages. Cell. Microbiol. **8:**1634–1642.
33. **Hu, T., S. Ramachandra Rao, S. Siva, C. Valancius, Y. Zhu, K. Mahadev, I. Toh, B. Goldstein, M. Woolkalis, and K. Sharma.** 2005. Reactive oxygen species production via NADPH oxidase mediates TGF-β-induced cytoskeletal alterations in endothelial cells. Am. J. Physiol. Renal Physiol. **289:**F816–F842.
34. **Ihara, S., T. Oka, and Y. Fukui.** 2006. Direct binding of SWAP-70 to non-muscle actin is required for membrane ruffling. J. Cell Sci. **119:**500–507.
35. **Kang, T., M. Fenton, M. Weiner, S. Hibbs, S. Basu, L. Baillie, and A. Cross.** 2005. Murine macrophages kill the vegetative form of *Bacillus anthracis*. Infect. Immun. **73:**7495–7501.
36. **Kassam, A., S. Der, and J. Mogridge.** 2005. Differentiation of human monocytic cell lines confers susceptibility to *Bacillus anthracis* lethal toxin. Cell. Microbiol. **7:**281–292.
37. **Katoh, M., and M. Katoh.** 2004. Identification and characterization of human FNBP1L gene in silico. Int. J. Mol. Med. **13:**157–162.
38. **Kawasaki, H., G. M. Springett, N. Mochizuki, S. Toki, M. Nakaya, M. Matsuda, D. E. Housman, and A. M. Graybiel.** 1998. A family of cAMP-binding proteins that directly activate Rap1. Science **282:**2275–2279.
39. **Kirby, J.** 2004. Anthrax lethal toxin induces human endothelial cell apoptosis. Infect. Immun. **72:**430–439.
40. **Komuro, I., N. Keicho, A. Iwamoto, and K. Akagawa.** 2001. Human alveolar macrophages and granulocyte-macrophage colony-stimulating factor-induced monocyte-derived macrophages are resistant to H_2O_2 via their high basal and inducible levels of catalase activity. J. Biol. Chem. **276:**24360–24364.
41. **Kumar, P., N. Ahuja, and R. Bhatnagar.** 2002. Anthrax edema toxin requires influx of calcium for inducing cyclic AMP toxicity in target cells. Infect. Immun. **70:**4997–5007.
42. **Lasunskaia, E., M. Campos, M. de Andrade, R. Damatta, T. Kipnis, M. Einicker-Lamas, and W. Da Silva.** 2006. Mycobacteria directly induce cytoskeletal rearrangements for macrophage spreading and polarization through TLR2-dependent PI3K signaling. J. Leukoc. Biol. **80:**1480–1490.
43. **Leppla, S.** 1982. Anthrax toxin edema factor: a bacterial adenylate cyclase that increases cyclic AMP concentrations of eukaryotic cells. Proc. Natl. Acad. Sci. USA **79:**3162–3166.
44. **Leppla, S., and P. Greengard.** 1984. Advances in cyclic nucleotide and protein phosphorylation research, p. 189–198. Raven Press, New York, NY.
45. **Loughran, G., N. Healy, P. Kiely, M. Huigsloot, N. Kedersha, and R. O'Connor.** 2005. Mystique is a new insulin-like growth factor-I-regulated PDZ-LIM domain protein that promotes cell attachment and migration and suppresses anchorage-independent growth. Mol. Biol. Cell **16:**1811–1822.
46. **Matsuda, S., K. Akagawa, M. Honda, Y. Yokota, Y. Takebe, and T. Takemori.** 1995. Suppression of HIV replication in human monocyte-derived macrophages induced by granulocyte/macrophage colony-stimulating factor. AIDS Res. Hum. Retrovir. **11:**1031–1038.
47. **May, R., and L. Machesky.** 2001. Phagocytosis and the actin cytoskeleton. J. Cell Sci. **114:**1061–1077.
48. **Nakata, K., K. Akagawa, M. Fukayama, Y. Hayashi, M. Kadokura, and T. Tokunaga.** 1991. Granulocyte-macrophage colony-stimulating factor promotes the proliferation of human alveolar macrophages in vitro. J. Immunol. **147:**1266–1272.
49. **Nakata, K., M. Weiden, T. Harkin, D. Ho, and W. Rom.** 1995. Low copy number and limited variability of proviral DNA in alveolar macrophages from HIV-1-infected patients: evidence for genetic differences in HIV-1 between lung and blood macrophage populations. Mol. Med. **1:**744–757.
50. **O'Brien, J., A. Friedlander, T. Dreier, J. Ezzell, and S. Leppla.** 1985. Effects of anthrax toxin components on human neutrophils. Infect. Immun. **47:**306–310.
51. **Paccani, S., F. Tonello, R. Ghittoni, M. Natale, L. Muraro, M. M. D'Elios, W. Tang, C. Montecucco, and C. Balderi.** 2005. Anthrax toxins suppress T lymphocyte activation by disrupting antigen receptor signaling. J. Exp. Med. **201:**325–331.
52. **Peterson, J., J. Comer, W. Baze, D. Noffsinger, A. Wenglikowskie, K. Walberg, J. Hardcastle, J. Pawlik, K. Bush, J. Taormina, S. Moen, J. Thomas, B. Chatuev, L. Sower, A. Chopra, L. Stanberry, R. Sawada, W. Scholz, and J. Sircar.** 2007. Human monoclonal antibody AVP-21D9 to protective antigen reduces dissemination of the *Bacillus anthracis* Ames strain from the lungs in a rabbit model. Infect. Immun. **75:**3414–3424.
53. **Popov, S., R. Villasmil, J. Bernardi, E. Grene, J. Cardwell, A. Wu, D. Alibek, C. Bailey, and K. Alibek.** 2002. Lethal toxin of *Bacillus anthracis* causes apoptosis of macrophages. Biochem. Biophys. Res. Commun. **293:**349–355.
54. **Preisz, H.** 1909. Experimentelle Studien åber Virulenz, Empfänglichkeit und 541 Immunität beim Milzbrand. Z. Immunität. Forsch. **5:**341–452.
55. **Razin, E., S. Bauminger, and A. Globerson.** 1978. Effects of prostaglandins on phagocytosis of sheep erythrocytes by mouse peritoneal macrophages. J. Reticuloendothel. Soc. **23:**237–242.
56. **Rossi, S., F. Tonello, L. Patrussi, N. Capitani, M. Simonato, C. Montecucco, and C. Baldari.** 2007. Anthrax toxins inhibit immune cell chemotaxis by perturbing chemokine receptor signaling. Cell. Microbiol. **9:**924–929.

57. **Scobie, H., G. Rainey, K. Bradley, and J. Young.** 2003. Human capillary morphogenesis protein 2 functions as an anthrax toxin receptor. Proc. Natl. Acad. Sci. USA **100:**5170–5174.
58. **Shinohara, M., Y. Terada, A. Iwamatsu, A. Shinohara, N. Mochizuki, M. Higuchi, Y. Gotoh, S. Ihara, S. Nagata, H. Itoh, Y. Fukui, and R. Jessberger.** 2002. SWAP-70 is a guanine-nucleotide-exchange factor that mediates signaling of membrane ruffling. Nature **416:**759–763.
59. **Takei, K., K. Tokuyama, M. Kato, and A. Morikawa.** 1998. Role of cAMP in reducing superoxide anion generation in guinea pig alveolar macrophages. Pharmacol. **57:**1–7.
60. **Tang, W., J. Krupinski, and A. Gilman.** 1991. Expression and characterization of calmodulin-activated (type 1) adenylylcyclases. J. Biol. Chem. **266:** 8595–8603.
61. **Voth, D., E. Hamm, L. Nguyen, A. Tucker, I. Salles, O. Ortiz-Leduc, and J. Ballard.** 2005. *Bacillus anthracis* oedema toxin as a cause of tissue necrosis and cell type-specific cytotoxicity. Cell. Microbiol. **7:**1139–1149.
62. **Welkos, S., A. Friedlander, S. Weeks, S. Little, and I. Mendelson.** 2002. *In vitro* characterization of the phagocytosis and fate of anthrax spores in macrophages and the effects of anti-PA antibody. J. Med. Microbiol. **51:**821–831.
63. **Wright, G., and G. Mandell.** 1986. Anthrax toxin blocks priming of neutrophils by lipopolysaccharide and by muramyl dipeptide. J. Exp. Med. **164:** 1700–1709.

Editor: S. R. Blanke